Journal of Solid State Chemistry **168,** 134–139 (2002)
doi:10.1006/jssc.2002.9700

Synthesis, Characterization, and Conductivity Studies of Poly-*o*-Methoxyaniline Intercalated into V_2O_5 Xerogel

Elídia M. Guerra,* Carlos A. Brunello,† Carlos F.O. Graeff,† and Herenilton P. Oliveira*,[1]

*Departamento de Química and †Departamento de Física e Matemática, FFCLRP, Universidade de São Paulo, Av. Bandeirantes 3900, 14040-901 Ribeirão Preto, Sao Paulo, Brazil

Received February 19, 2002; in revised form July 15, 2002; accepted July 18, 2002

In this work we study the conductivity properties of poly-*o*-methoxyaniline/V_2O_5 intercalation compounds obtained through intercalative polymerization of *o*-methoxyaniline with $V_2O_5 \cdot nH_2O$ in hydrogel form and by reacting directly with V_2O_5 film in de-hydrated form (xerogel). These new compounds were characterized using Fourier-transform infrared and ultraviolet/visible spectroscopies, electron paramagnetic resonance, elemental analysis (C, N, H), thermogravimetric analysis, scanning electron microscopy, dc-conductivity and powder X-ray diffraction. For samples formed from V_2O_5 xerogel in film form, an increase in dc-conductivity and a decrease in the thermal activation energy in comparison with pure matrix was observed. The increase in conductivity is attributed to an increase of carrier density in the vanadium oxide lattice and the contribution of polarons from the polymer. On the other hand, for the intercalation compound obtained with $V_2O_5 \cdot nH_2O$ in hydrogel form presents a very low room temperature conductivity value. The decrease in conductivity is due to the lack of connectivity of the various parts that compose the material. © 2002 Elsevier Science (USA)

Key Words: **vanadium pentoxide; poly-*o*-methoxyaniline; intercalation.**

INTRODUCTION

In situ intercalation/polymerization of polymer precursors into suitable host structures has been widely used to obtain multiphase materials containing two or more components mixed at the nanometer scale with unique properties (1–3). The synergic effect resulting from the combined properties of organic–inorganic components can give rise to very interesting features, especially in what concerns electrochemical, electrochromic and conduction properties (1–3). In particular, intercalation of conducting organic polymers (polyaniline and polythiophene, e.g.) into inorganic matrices has been the focus of numerous works (1, 3–5). Taking advantage of the vanadium pentoxide xerogel's bi-dimensional structure (6), it is possible to synthesize several different intercalation compounds in which the guest species can vary from simple ions to polymeric species (1, 5–7). There are several reports dealing with the V_2O_5/polyaniline system (5, 7–9) investigating its conductivity and electrochemical properties and the influence of synthesis methodology on the resulting properties, however, systems with polyaniline derivative have been receiving less attention (10–12). In this paper, intercalation of poly *o*-methoxyaniline (POMA) into vanadium pentoxide matrix has been performed. POMA was chosen due to the presence of methoxy groups that increase the inter-chain separation and intra-chain disorder as well as POMA presents high solubility in common organic solvents improving its processability (13–15). In particular, our interest is to investigate the conductivity properties of the intercalation compounds resulting from the presence of POMA in the interlayer domain of the host structure. Moreover, we also studied the influence of different morphological structures on conductivity due to the different synthetic methodologies used to obtain the materials: by reacting the monomer with vanadium pentoxide in hydrogel form ($V_2O_5 \cdot nH_2O$) and in xerogel film form ($V_2O_5 \cdot 1.9H_2O$).

EXPERIMENTAL SECTION

Reagents

The monomer, *o*-methoxyaniline (Aldrich), was purified by vacuum distillation before use and all other chemicals used were reagent grade and were used without any previous treatment. Vanadium pentoxide xerogel was prepared from sodium metavanadate (Fluka) and the ion-exchange resin used was Dowex-50X in acid form. Water was purified using a Millipore Milli-Q System.

---

[1] To whom correspondence should be addressed. Fax: +55-16-633-8151. E-mail: herepo@ffclrp.usp.br.

0022-4596/02 $35.00

Synthesis of V_2O_5/POMA Intercalation Compounds

Vanadium pentoxide gel, $V_2O_5 \cdot nH_2O$, was prepared by ion-exchange method (16) from $0.1\,\mathrm{mol\,L^{-1}}$ aqueous solution of sodium metavanadate. The synthesis of the intercalation compounds was carried out by using two routes: reacting *o*-methoxyaniline with vanadium pentoxide in hydrogel form (GF) and; reacting the monomer with vanadium pentoxide xerogel in film form (FF). The former was performed as follows: we reacted 15 mL of the vanadium pentoxide gel with 10 mL of a solution containing 4.0×10^{-3} mol of *o*-methoxyaniline dissolved in 100 mL of $2.0 \times 10^{-2}\,\mathrm{mol\,dm^{-3}}$ H_2SO_4 aqueous solution, under stirring during 24 h and at room temperature (22°C). The resulting suspension was cast into film form by the slow evaporation of water on a substrate (glass plate) at room temperature in air, leading to a dark blue film, and finally rinsed with purified water and dried again (sample GF-1). The resulting film has a powder-like morphology. The latter method consisted of a reaction between 4.5×10^{-2} mol (~ 10 mg) of vanadium pentoxide xerogel in FF ($V_2O_5 \cdot 1.9H_2O$), prepared on a glass plate, with 5.0 mL of 2.0×10^{-3} mol (sample FF-1) and with 5.0 mL of 4.0×10^{-3} mol (sample FF-2) of *o*-methoxyaniline dissolved in 100 mL of $2.0 \times 10^{-2}\,\mathrm{mol\,dm^{-3}}$ H_2SO_4 aqueous solution. The mixture was allowed to stand at room temperature (22°C) in air until the solvent was evaporated. The films obtained were rinsed with $1.0 \times 10^{-3}\,\mathrm{mol\,dm^{-3}}$ H_2SO_4 aqueous solution followed by water and dried at room temperature. The products exhibited a metallic, dark blue color. The samples were removed from the glass plate and stored under vacuum. Note that the intercalation of POMA with vanadium pentoxide is a redox reaction in which POMA is oxidatively polymerized concomitantly with the reduction of vanadium oxide, thus the blue color is associated with vanadium in its reduced form (V^{IV}) and the color does not disappear after rinsing. The compositions of the compounds were determined by elemental analysis and by thermogravimetric analysis. The obtained values were as follows:

Sample FF-1: $(V_2O_5)_{1.0}(\mathrm{POMA})_{0.71}(H_2O)_{0.94}$;
Sample FF-2: $(V_2O_5)_{1.0}(\mathrm{POMA})_{1.0}(H_2O)_{0.87}$;
Sample GF-1: $(V_2O_5)_{1.0}(\mathrm{POMA})_{1.3}(H_2O)_{1.0}$.

It should be noted that despite the reactions being carried out in H_2SO_4 med, the presence of sulfur (performed by elemental analysis) in the materials was not evidenced indicating that sulfate ions were eliminated during rinsing.

Equipment and Procedure

Elemental analysis (carbon, nitrogen, hydrogen and sulfur content) was performed using an Elemental Analyzer CE Instruments, model EA-1110 obtained by the Dynamic Flash Combustion method. The thermogravimetric data were registered on a Thermal Analyst equipment model 2100-TA in air atmosphere and at a heating rate of $10°\mathrm{C\,min^{-1}}$. The powder X-ray diffraction (PXRD) data were recorded on a SIEMENS D5005 diffractometer using a graphite monochromador and Cu$K\alpha$ emission lines (1.541 Å, 40 kV, 40 mA) with the samples, in film form, deposited onto a glass plate, and the data were collected at room temperature over the range of $2° \leq 2\theta \leq 50°$ with a step of 0.020°. Fourier-transform infrared spectra (FTIR) were recorded from 2000 to $400\,\mathrm{cm^{-1}}$ on a Bomem MB 100 spectrometer and the samples were dispersed in KBr and pressed into pellets. The transmission electronic spectra (ultraviolet/visible spectra, UV/Vis) were recorded on a Varian Cary 50 spectrophotometer. For the sample GF-1, 10 μL of the suspension was cast on a quartz plate of $0.7\,\mathrm{cm^2}$ followed by evaporation of solvent and rinsing with water, and then the measurement was performed. Electron paramagnetic resonance (EPR) spectra were obtained at room temperature using a computer interfaced Varian E-4 spectrometer operating at 9.5 GHz (X band). Scanning electronic microscopy (SEM) studies were done on a ZEISS - DSM 940 microscope, operating at 20 kV. For the sample GF-1, 20 μL of the suspension was cast on an aluminum sample plate holder followed by evaporation of solvent and rinsing with water. For samples FF-1 and FF-2, they were fixed on an aluminum support with silver glue. All samples received a gold coating before measurements. DC conductivity was measured against temperature in the 150–350 K range. The conductivity studies were performed as two points measurements in an evacuated chamber using a dc bias of 1 V between silver electrodes, and the reproducibility of the experiments was tested twice for each sample. The samples were deposited in film form on a glass plate ($0.8 \times 0.8\,\mathrm{cm^2}$) in order to maintain the same thickness.

RESULTS

Figures 1a–d show the typical powder X-ray diffraction patterns for the vanadium pentoxide xerogel matrix and for the V_2O_5/POMA compounds. For all intercalation compounds, the diffraction patterns present broad and low intensities peaks, suggesting a decrease in crystallinity with respect to the matrix. In addition, the shifts of 001 reflections to lower 2θ values indicate an increase of the interlayer spacing consistent with the presence of the polymeric species inside the matrix (*d*-spacing of 1.19 nm): *d*-spacing equal to 1.44 nm for samples FF-1 and FF-2 and equal to 1.65 nm for sample GF-1.

Figure 2 shows FTIR spectra of intercalation compounds as well as the spectrum of the vanadium pentoxide xerogel matrix. The spectra of the new compounds present

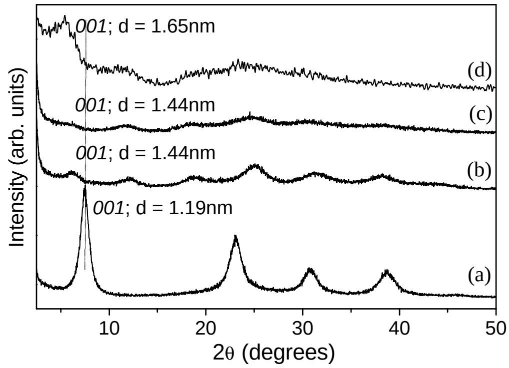

FIG. 1. Powder X-ray diffraction patterns of the hydrated vanadium pentoxide matrix (a), sample FF-1 (b), sample FF-2 (c) and sample GF-1 (d).

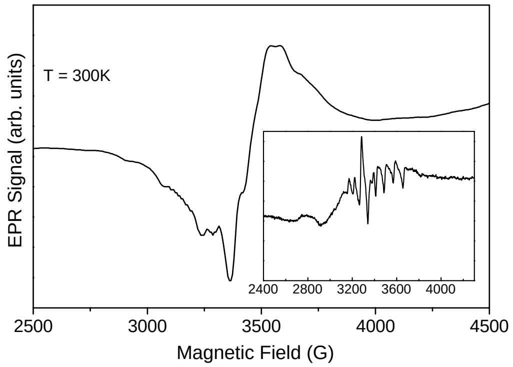

FIG. 3. EPR spectra of the sample FF-2, $(V_2O_5)_{1.0}(POMA)_{1.0}(H_2O)_{0.87}$, in film form and at room temperature (24°C) and of the hydrated vanadium pentoxide matrix ($V_2O_5 \cdot 1.9H_2O$), inset.

the typical bands of the matrix: $1010.0\,cm^{-1}$, $\nu(V{=}O)$; $763.7\,cm^{-1}$, $\nu(V{=}O)$; $531.6\,cm^{-1}$, $\delta(V{=}O)$. Despite the slight shifts of these bands in relation to the matrix, we can suppose that the overall framework is preserved after the reaction, in agreement with the powder X-ray diffraction data. In addition, the new compounds' spectra clearly show the presence of the characteristic vibrational modes attributed to the organic phases (17, 18): $1118\,cm^{-1}$, δ(CH); $1167\,cm^{-1}$, δ(CH); $1207\,cm^{-1}$ and $1260\,cm^{-1}$, ν(CN) of C-N single bands; $1294\,cm^{-1}$, ν(CN), and; $1456\,cm^{-1}$ and $1490\,cm^{-1}$, ν(CC) related to benzene rings.

Figure 3 shows typical EPR spectra of the matrix and of the intercalation compound (sample FF-2). The EPR signal from hydrated vanadium pentoxide matrix (Fig. 3, inset) comes from $V^{(IV)}$ ($S = \frac{1}{2}, I = \frac{7}{2}$) centers, with the characteristic hyperfine structure in a axially distorted crystal field. The broad signal centered around $g = 1.97$, verified in the spectrum of new material (Fig. 3), reflects the reduction state of V^{V}, or the increase in V^{IV} concentration (16, 195). In other words, the reaction between the host specie and the monomer induces the reduction of the V^{V} ions to V^{IV}. It should be noted that in the intercalated samples, no signal coming from organic polymer could be observed. The ESR signal coming from POMA is assigned to free polarons, thus either there is a decrease in the number of free polarons, or the ESR lineshape from POMA is broadened due to the presence of paramagnetic V ions, which makes its detection more difficult.

The ultraviolet/visible electronic spectra of both the vanadium pentoxide xerogel matrix and the intercalation compound obtained through the reaction with the matrix in hydrogel form (sample GF-1) are shown in Fig. 4. The UV/Vis a spectrum of the free matrix, before the intercalation, presents an absorption band at 380 nm, which is due to the vanadium(V)-oxide charge-transfer bands (162). The intercalated POMA compound exhibits two bands at 315 and 411 nm and a shoulder around 550 nm. The two former bands correspond to the $\pi \rightarrow \pi^*$ transition of conjugated benzenoid rings of polymer. The latter is ascribed to an exciton-like transition of quinone diimine moiety (17–19).

From scanning electron micrographs of the matrix and of the intercalation compounds, shown in Fig. 5, we can note a morphological difference among the products

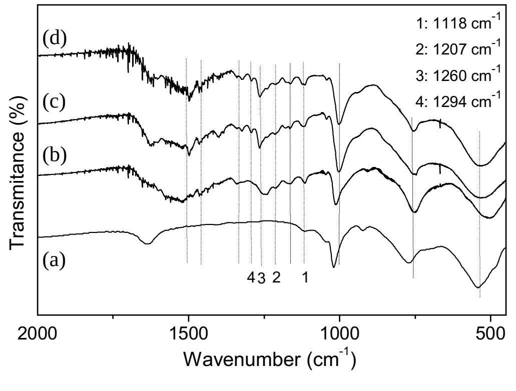

FIG. 2. FTIR of the hydrated vanadium pentoxide matrix (a), sample FF-1 (b), sample FF-2 (c) and sample GF-1 (d).

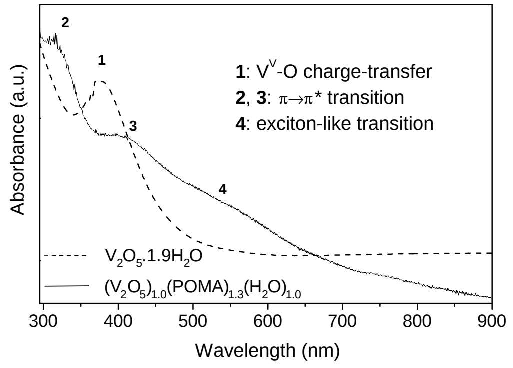

FIG. 4. UV/Vis spectra of the hydrated vanadium pentoxide matrix (a) and the intercalated compound $(V_2O_5)_{1.0}(POMA)_{1.3}(H_2O)_{1.0}$, sample GF-1.

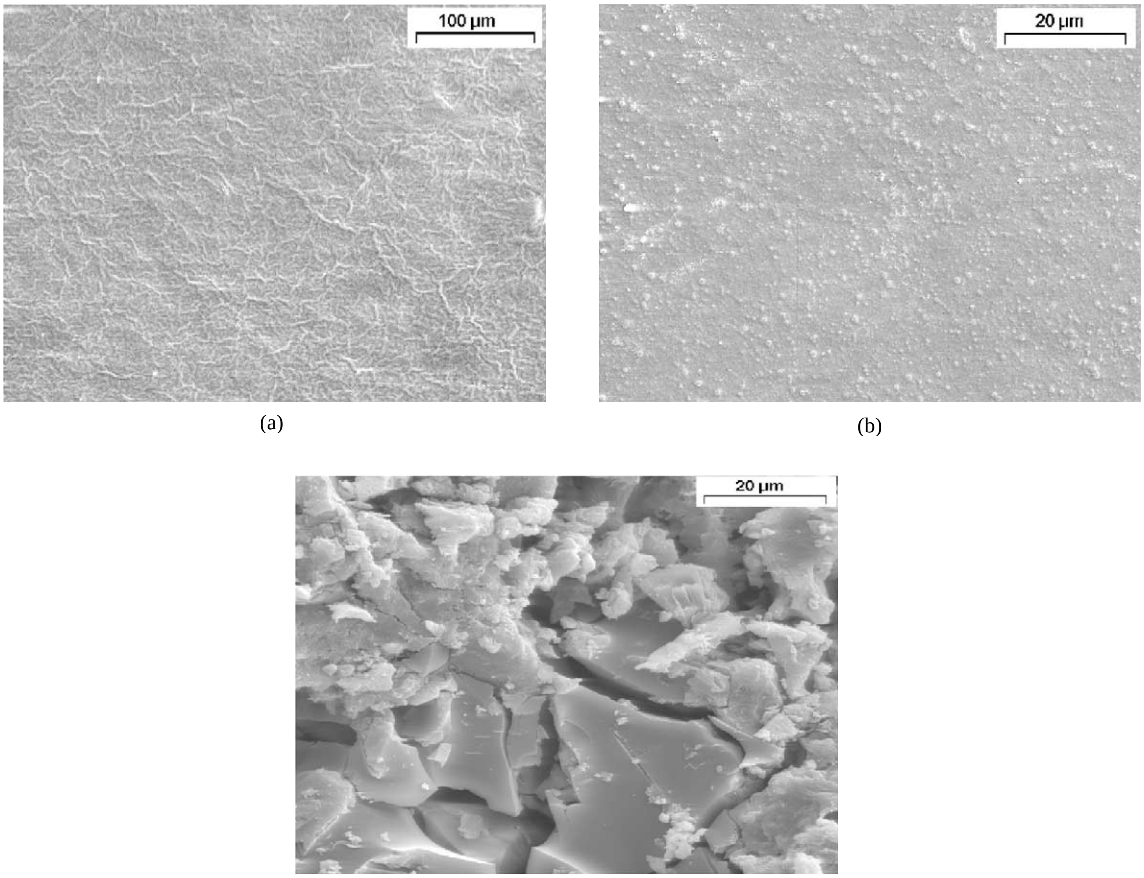

(a) (b)

(c)

FIG. 5. Scanning electron micrographs of the hydrated vanadium pentoxide matrix (a), sample FF-1 (b) and sample GF-1 (c).

obtained from different synthetic procedures utilized. Vanadium pentoxide xerogel films (Fig. 5a) presents fibers and ribbons that are interconnected, forming a network of chains with a fibrous texture (20). The intercalation compounds formed by the reaction between the monomer and the matrix in film form (sample FF-1) present a continuous surface, as shown in Fig. 5b, however, the morphology is better described by a rough surface rather than a fibrous texture. In contrast, the SEM image of material formed by the reaction with the matrix in hydrogel form (sample GF-1, shown in Fig. 5c) shows a dramatic change in morphology, from a network of chains to a structure formed by irregular aggregates with different sizes.

The presence of POMA changed the conductivity of the pure matrix, as shown in Fig. 6. The thermal activation energy decreased from 0.33 ± 0.07 eV in $V_2O_5 \cdot 1.9H_2O$ to 0.10 ± 0.02 eV in sample FF-1, 0.11 ± 0.02 eV in sample FF-2 and 0.12 ± 0.02 eV in sample GF-1. The room temperature conductivity did also change from $1.4 \pm 0.3 \times 10^{-4}$ $(\Omega\,\mathrm{cm})^{-1}$ in the pure matrix to $2.1 \pm 0.4 \times 10^{-1}$ $(\Omega\,\mathrm{cm})^{-1}$, $5.2 \pm 0.9 \times 10^{-2}$ $(\Omega\,\mathrm{cm})^{-1}$, $4.3 \pm 0.8 \times 10^{-5}$ $(\Omega\,\mathrm{cm})^{-1}$ for samples FF-1, FF-2 and GF-1, respectively. Moreover, in all cases the variation of conductivity with temperature has a thermally activated behavior.

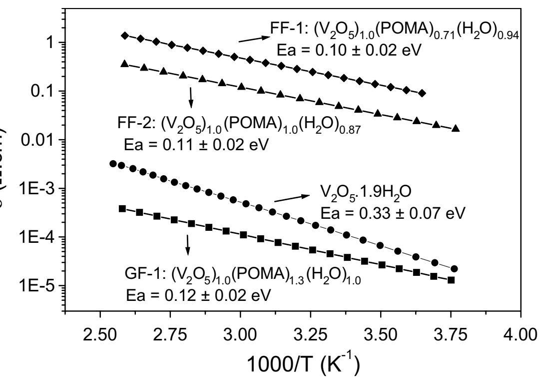

FIG. 6. DC conductivity measurements of the hydrated vanadium pentoxide matrix (-●-●-), sample FF-1 (-◆-◆-), sample FF-2 (-▲-▲-) and sample GF-1 (-■-■-).

DISCUSSION

The diffraction patterns of the obtained materials are consistent with a lamellar structure related to the presence of 001 reflections and in agreement with a topotactic mechanism. The increase of *d*-spacing is an evidence of the replacement of the interlamellar water molecules (weakly bounded) by poly *o*-methoxyaniline. In addition, as the increase of *d*-spacing was about 0.25–0.44 nm, it is supposed that a single layer of POMA is inserted in the interlayer domain; otherwise we should verify an increase of about 1.0 nm (3). It is important to note that not all the interlamellar water molecules were substituted by the polymer, as evaluated by elemental analysis and by thermogravimetric analysis. Thus, in the interlamellar domain, both water and organic molecules can coexist. Another point is that the intercalation compound formed by reacting the monomer with vanadium pentoxide in hydrogel form presents a low crystallinity (Fig. 1d), evidenced by broad and low intensity diffraction peaks, in comparison with the matrix in film form (Figs. 1b and 1c). Our results indicate that the reaction between the monomer and vanadium pentoxide in hydrogel form (GF) does not allow the formation of a network of interconnected chains producing a ribbon-like structure linked by hydrogen bonded water molecules. One possible explanation for this effect is that we noticed that the reaction occurs very fast, i.e., almost instantly upon contact of both reagents, forming insoluble aggregates and even after the de-hydration by slow evaporation of solvent, the typical lamellar structure of V_2O_5 is only partially retained. On the other hand, when the vanadium xerogel film is exposed to POMA, the structural integrity of V_2O_5 xerogel acts as a template during the reaction. As a consequence the overall host structure is partially retained. As the POMA concentration increases, a decrease in crystallinity is observed (Fig. 1c).

In Fig. 2, the band at 1118 cm^{-1} is observed in all spectra of the intercalation compounds, assigned to the CH in plane deformations vibrations (17, 18). This result is evidence that the poly-*o*-methoxyaniline formed in the interlayer spacing is partially oxidized. The band at 1294 cm^{-1} is assigned to ν(CN) of groups with partially double bonds order, probably due to the acid character of the matrix that can contribute to the conductivity of the organic polymer. The bands at 1207 cm^{-1} and 1260 cm^{-1} are characteristic of POMA in its insulating form. Thus, these observations suggest the coexistence of polymers in both insulating and conductive forms. From what has been discussed, FTIR spectra of intercalation compounds indicate that POMA was produced during the reaction with vanadium pentoxide in both film and hydrogel forms (17, 18). Wu *et al.* (7) have described that the process of polymerization/intercalation of aniline into vanadium pentoxide xerogel comprises several reaction steps such as oxidative polymerization of aniline and insertion of aniline/anilinium in the host lattice. We believe that in our case a similar mechanism occurs. The process starts when the matrix in film form is in contact with the solvent. The solvent swells the host specie, followed by the insertion of protonated monomers and ionic exchange reactions with protons already present in the interlamellar domain. Concomitantly and sequentially, occurs the oxidation of the monomer with the reduction of V_2O_5 matrix (V^{V} to V^{IV} evidenced by EPR signal, Fig. 3) and the growth of the polymeric units, resulting in a new material involving these two species. Note that, in the UV/Vis spectrum of the intercalation compound (Fig. 4), the absence of the band at 380 nm attributed to vanadium(V)-oxide CT transition is also an evidence that the reduction of metallic center to V^{IV} occurred, in agreement to EPR technique. In the case of reaction with vanadium pentoxide hydrogel, presumably, the synthesis is based on a modular process, in which, during the evaporation of the solvent, the organic and the inorganic units are assembled by self-organization. In order to attain this structure, probably the release of water molecules bounded to vanadium oxide promoted the increase of the hydrogen and van der Waals bonds between the organic and inorganic units that resulted in stable weak non-covalent and non-directional guest–host interactions (4, 21).

As already mentioned, the intercalated material FF-1 and FF-2, has a higher conductivity when compared to V_2O_5 matrix, with the exception of sample GF-1 that has a lower conductivity than the matrix. The increase in conductivity is probably due to an increase in $V^{IV}/(V^{IV} + V^{V})$ ratio in the host specie that becomes an n-doped electrically conductive mixed valence oxide (3), observed by EPR technique (Fig. 3). Thus, the conductivity values of intercalation compounds FF-1 and FF-2 have the contribution from the increase of hopping process of unpaired electron between metallic ions in different valence states found on the vanadium oxide xerogel lattice. In analogy, after the insertion and polymerization of *o*-methoxyaniline, the polymer is present in its doped form (*p*-doped), promoting the charge transport by polaronic species on the polymer backbone. Moreover, the absorption band of around 550 nm attributed to excitonic transition can be related to the charge caries responsible for the conductivity in the organic polymer (17, 18, 22), as shown in Fig. 4. So, we can infer that the conductivity in these materials depends on a double conduction mechanism: electron hopping process in the matrix; and polaron transport along the polymer backbone. Note that the conductivity values of these materials have almost the same magnitude in comparison with V_2O_5–polyaniline system (7, 23, 24). We could expect low conductivity values because of the combination of increased inter-chain separation and intra-chain disorder, as pointed out by Mergulhão and coauthors (13), leading to a decrease in effective conjugation of the polymer (14). However, the experimental data indicated, at least, that these aspects did not have any influence on the conductivity of this hybrid compound. At this point we are unable to draw any final conclusions and more studies are now underway in our laboratory. Another interesting feature is that the conductivity values of the final materials decrease when increasing the polymer content (for samples FF-2 and GF-1). One possible explanation is the fact that the polymer is in excess, so there is a higher content in its non-conductive form contributing to low values of conductivity. Besides, it is important to note that there is a strong dependence of sample morphology on conductivity. The material obtained by reacting the monomer with host species in gel form presents a very low room conductivity value (4.3×10^{-5} $(\Omega\,\mathrm{cm})^{-1}$) in comparison with the other samples. This effect can be explained from a morphological point of view, i.e., the sample is constituted by aggregates with different sizes (Fig. 5c) affecting the connectivity of particles, in contrast with intercalation compounds in film form, which presents a smooth surface (Fig. 5b).

CONCLUSIONS

In this work, the reaction between *o*-methoxyaniline with vanadium pentoxide matrix in xerogel and in hydrogel forms have been studied. The intercalated compounds obtained preserve the host structure integrality; however, the former presents a higher crystallinity degree, in agreement with PXRD data and SEM images. The synthesis process also affected the conductivity. For samples formed from V_2O_5 xerogel in film form, an increase in dc-conductivity was observed and a decrease in the thermal activation energy in comparison with pure matrix. The increase in conductivity is attributed to an increase of carrier density in the vanadium oxide lattice and the contribution of polarons from the polymer. On the other hand, a decrease in room temperature conductivity was verified in the intercalation compound obtained with the matrix in hydrogel form. The decrease in conductivity is due to the lack of connectivity of the various parts that compose the material.

ACKNOWLEDGMENTS

This work was supported by FAPESP (process 01/01527-5), CNPq and PIBIC/USP/CNPq.

REFERENCES

1. C. O. Oriakhi, *J. Chem. Educ.* **77**(9), 1138–1146 (2000).
2. P. Judeinstein and C. Sanchez, *J. Mater. Chem.* **6** (40), 511–525 (1996).
3. P. Gomez-Romero, *Adv. Mater.* **13,** 163–174 (2001).
4. E. Giannelis, *in* "Materials Chemistry—An Emerging Discipline" (L. V. Interrante, L. A. Caspar, and A. B. Ellis Eds.), Advances in Chemistry Series 245, p. 259. American Chemical Society, Washington, DC, 1995.
5. F. Leroux, G. Goward, W. P. Power, and L. F. Nazar, *J. Electrochem. Soc.* **144,** 3886–3895 (1997).
6. J. Livage, *Coord. Chem. Rev.* **178–180,** 999–1018 (1998).
7. C.-G. Wu, D. C. DeGroot, H. O. Marcy, J. L. Schindler, C. R. Kannewurf, Y.-J. Liu, W. Hirpo, and M. G. Kanatzidis, *Chem. Mater.* **8,** 1992–2004 (1996).
8. M. G. Kanatzidis, C. G. Wu, H. O. Marcy, and C. R. Kannewurf, *J. Am. Chem. Soc.* **111,** 4139–4141 (1989).
9. M. Lira-Cantú and P. Gómez-Romero, *Int J. Inorg. Mater.* **1,** 111–116 (1999).
10. F. Huguenin, M. T. D. Gambardella, R. M. Torresi, S. I. de Torresi, and D. A. Buttry, *J. Electrochem. Soc.* **147,** 2437–2444 (2000).
11. W. ChunGuey, H. J. Yih, and H. Shuisheng, *J. Mater. Chem.* **11,** 2061–2066 (2001).
12. F. Huguenin, M. J. Giz, E. A. Ticianelli, and R. M. Torresi, *J. Power Sources* **103,** 113–119 (2002).
13. S. Mergulhão, R. M. Faria, G. F. L. Ferreira, and J. Sworakowski, *Chem. Phys. Lett.* **269,** 489–493 (1997).
14. A. Paul, T. N. Misra, and D. Talukdar, *Solid State Commun.* **99,** 633–636 (1996).
15. D. Gonçalves, L. H. C. Mattoso, and L. O. S. Bulhões, *Electrochim. Acta* **39,** 2271–2275 (1994).
16. N. Gharbi, C. Sanchez, J. Livage, J. Lemerle, L. Nejem, and J. Lefebvre, *Inorg. Chem.* **21,** 2758–2765 (1982).
17. J. Widera, B. Palys, J. Bukowska, and K. Jackowska, *Synth. Metals* **94,** 265–272 (1998).
18. A. Grugeer, A. Novak, A. Régis, and Ph. Colomban, *J. Mol. Struct.* **328,** 153–167 (1994).
19. W. A. Gazotti Jr., M. J. D. M. Jannini, S. I. Córdoba de Torresi, and M.-A. De Paoli, *J. Electroanal. Chem.* **440,** 193–199 (1997).
20. H. P. Oliveira, C. F. O. Graeff, and J. M. Rosolen, *Mater. Res. Bull.* **12–13,** 1891–1903 (1999).
21. F. Babonneau, P. Barboux, F. A. Josien, and J. Livage, *J. Chim. Phys.* **82,** 761–766 (1985).
22. F. A. Viva, E. M. Andrade, F. V. Molina, and M. I. Florit, *J. Electroanal. Chem.* **471,** 180–189 (1999).
23. H. P. Oliveira, C. F. O. Graeff, C. A. Brunello, and E. M. Guerra, *J. Non-Cryst. Solids* **273,** 193–197 (2000).
24. M. Lira-Cantú and P. Gómez-Romero, *J. Solid State Chem.* **147,** 601–608 (1999).